Available online at www.sciencedirect.com

SciVerse ScienceDirect

Procedia Engineering 36 (2012) 212 – 216

Procedia Engineering

www.elsevier.com/locate/procedia

IUMRS-ICA 2011

High Temperature Corrosion Behaviors of the Superheater Materials

Wen-Wen Luo[a,*] , Zong-De Liu[a,b], Yong-Tian Wang[a], Rong-Juan Yang[a]

[a]*Key Laboratory of Condition Monitoring and Control for Power Plant Equipment of Ministry of Education,North China Electric Power University,Beijing 102206,China*

[b]*Suzhou Institute of Research，North China Electric Power University, NO.188, Renai Road, Xietang area, Suzhou 215123,China*

Abstract

The high temperature corrosion tests are performed on 20#steel, TP347H and superalloy C22. The high temperature corrosion behaviors of these superheater materials in the synthetic salt containing 80wt-%KCl+20wt-%K_2SO_4 have been investigated under the oxidizing atmosphere at a temperature of 650℃ for 218 hours. For comparison, the column diagram has been obtained by mass loss. The scanning electron microscopy (SEM) with energy dispersive spectrometer (EDS) is used to characterize the surface morphology and compositions of the corrosion products. The results have shown that the superalloy C22 exhibits the high corrosion resistance.

Keywords: High-temperature corrosion; the superalloy C22; TP347H; 20#steel

1. Introduction

Global warming concerns have, in recent years, fostered interest in CO_2-neutral energy sources for power production. Biomass is a renewable resource with almost zero net CO_2 emission since carbon and energy are sequestered during the biomass growth [1-2]. Furthermore, considering the present technical level and economics, biomass is cheap and easy to use. Traditionally, biomass-fired boilers have not experienced great problems with high-temperature corrosion, because the metal temperature of the superheater tubes has been mainly kept low (in Denmark below 450℃). However, in order to improve the

* Corresponding author. Tel.: +86-10-6177-2291; Fax: +86-10-6177-2812.
E-mail address: luowenwen@ncepu.edu.cn.

1877-7058 © 2012 Published by Elsevier Ltd. Open access under CC BY-NC-ND license.
doi:10.1016/j.proeng.2012.03.033

electrical efficiency of the biomass fired plants, a desire to raise the temperature of the superheated steam has introduced the potential high-temperature corrosion problems.

Biomass has a high content of alkali metals and chlorine, and most biomass fuels contain very little sulphur. In particular, the high content of potassium and chlorine in deposits formed during the combustion of straws and grasses are potentially harmful elements with regard to corrosion of heat transfer surfaces. Biomass deposits usually have a high content of potassium, silicon, and calcium, but may also be rich in sulfur and chlorine. Especially the deposits from the straw-fired plants have high chlorine content [3-5]. Baxter et al. [3] have reported the chlorine contents in the superheater deposits from two Danish straw-fired plants in the range of 23–26 wt.%. Chlorine contents as high as 38 wt.% are found in furnace deposits from a Danish straw-fired grate [5]. Data on typical fuel compositions and on ash formation are reported in a number of works [6-8].

The chlorine-containing ash deposits accelerate the corrosion by several mechanisms. A common hypothesis regarding chlorine-induced high-temperature corrosion is the chlorine in the form of alkali chloride at a steel surface at temperatures higher than 450℃ actively increases the oxidation of the steel surface [9-10]. The process is named in some cases as “active oxidation” in which a “chlorine cycle” is assumed to be involved. Especially the role of potassium has been alighted with the identification of potassium chromate in the corrosion layer [11-12].

The problem of high temperature corrosion is a crucial impediment for the commercialization of biomass fired power generation. From this it follows that there is a need to investigate the corrosion resistance of different superheater materials to high temperature corrosion.

2. Experimental

2.1. Sample preparation

The tested materials are 20#steel, which have Ni–Cr contents of 0.5 wt.% and TP347H with Ni–Cr contents of 26~31 wt.% as well as the superalloy C22, which have Ni–Cr contents of 78 wt.%. The compositions of the tested materials are given in Table 1.

Table 1. The compositions of the tested materials.

Element (wt-%)	Ni	Cr	Mo	Mn	Si	C	W	Cu	S	P
20#steel	≤0.25	≤0.25	0	0.35~0.65	0.17~0.37	0.17~0.24	0	≤0.25	≤0.04	≤0.04
TP347H	8.00~11.00	18.00~20.00	0	≤2.00	≤0.75	0.04~0.10	0	—	≤0.03	≤0.04
C22	56	22	13	≤0.5	≤0.08	≤0.01	3	≤0.5	0	0

The samples are cut into approximately 15×10×2 mm and ground with 800 grit SiC paper. Afterwards, the samples are cleaned and degreased with acetone in an ultrasonic bath and subsequently weighed using an electronic scale with a precision of 0.1 mg.

2.2. High temperature corrosion test

The specimens are completely immersed into a crucible with synthetic salt containing 80 wt.% KCl + 20wt.% K_2SO_4 under oxidizing environment (air). The crucible with samples is then put into a furnace running at 650℃. After 218 hours, the specimens are withdrawn from the crucible, cooled in air, cleaned with a soft brush, washed in boiling water for removing the salt left on the surface, and dried in hot air.

Fig.1 is a schematic drawing showing the setting of the testing method.

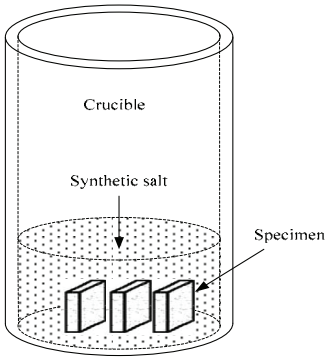

Fig. 1. Schematic drawings of high temperature corrosion test settings: The specimens are immersed in the synthetic salt.

Then the corrosion products are removed by chemical treatment and subsequently the mass loss is determined. The analysis of the corrosion degree is conducted by valuing the surfaces, which are ultrasonically degreased in acetone, then blow dry.

3. Results and Discussion

3.1. Mass losses of tested materials in high temperature exposure tests

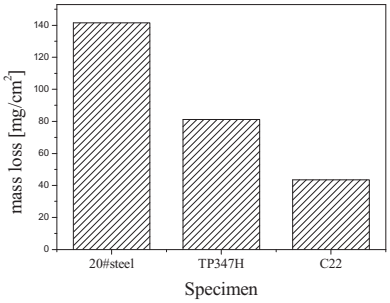

Fig. 2. Mass losses of the specimen (comparison of corrosion rates of materials).

The mass losses of materials which are tested in synthetic salt are shown in Fig. 2. As the results show, the corrosion rate of materials decreases from 20#steel to TP347H and the superalloy C22 in turn. The Cr content of 20#steel, TP347H and the superalloy C22 is ~0.25, 18.0~20.0 and 22 wt-% and the Ni content is 0.25, 8.0~11.0 and 56 wt-%, respectively. It is known that alloy with chromium [13] and Ni will increase the corrosion resistance of steels, so the corrosion resistance of 20#steel is the lowest, followed by that of TP347H and the superalloy C22. In conclusion, the corrosion resistance of material increases mainly with the increase of the Ni/Cr content.

3.2. The SEM of corrosion products in high temperature exposure tests

One piece of each sample material immersed into the synthetic salt is additionally exposed for SEM-EDX analysis. The corrosion degrees are analyzed by observation of surfaces. Fig. 3 shows the selected SEM images of the corrosion products of the tested samples.

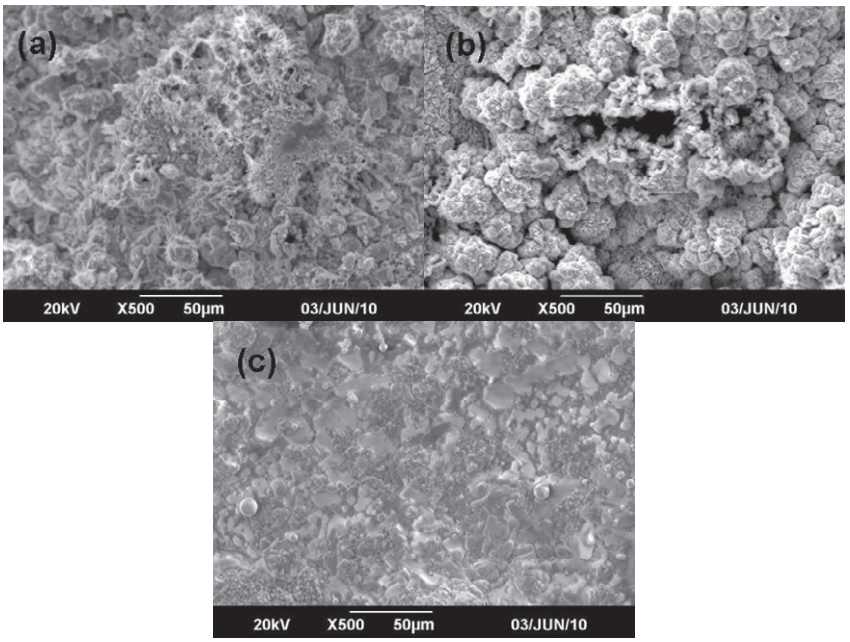

Fig.3. SEM micrographs of specimen after the 218 hours exposure immersed in molten salt at 650℃; (a) 20#steel; (b) TP347H; (c) the superalloy C22.

The corrosion product on 20#steel is shown in Fig. 3a. The 20# steel suffers severe corrosion at the surface. Plenty of iron and oxygen are detected in the disintegrated oxide layers. The oxide layers are extensively spalled, which are thick, porous and non-protective. Fig. 3b shows the SEM image of corrosion products on TP347H. The oxide layers consist of the mixed Ni, Fe and Cr oxides. In addition to pure iron oxide, the oxides on TP 347H are mixed, e.g. iron oxide mixed with chromium. Compared with 20#steel and TP347H, the surface of the superalloy C22 is more stable, even at 650℃. Mixed oxides with Ni, Fe and Cr are formed on it, and the oxide layers contain also plenty of alkali salts. The corrosion products of the superalloy C22 are presented in Fig. 3c.

To conclude, the mainly detected oxides detected are Fe–O on 20#steel, Fe–O–Cr–(Mn) on TP347H and Ni–Cr–Fe–O on the superalloy C22. In addition, the corrosion scale of 20#steel is lamellar and porous as a result it is brittle partially and the corrosion scale of TP347H is porous while the corrosion scale of the superalloy C22 is fine and light, all of these results correspond proportionally to the mass losses (Fig.2).

4. Conclusions

The high temperature corrosion of three superheater materials is examined in the tests immersed into

synthetic salt containing 80 wt.% KCl + 20 wt.% K_2SO_4 for 218 h at 650℃ and subsequently the mass loses of materials are determined and the corrosion products are analyzed by SEM-EDX.

The results can be summarized as follows:

- The rate of mass loss decreases from 20#steel to TP347H and the superalloy C22.
- The corrosion degree of each specimen corresponds proportionally to the mass losses.

The corrosion resistances of superheater materials depend on the Ni/Cr content, which have positive influence on the corrosion behavior. Thereby the superalloy C22 has the highest resistance, followed by TP347H and 20#steel.

Acknowledgements

This project was supported by the Scientific and Technological Achievements Transformation and Industrialization of Beijing Municipal Education Commission, the Suzhou Municipal Science and Technology Plan Project (Grant No.SYG201002), the National Natural Science Foundation of China (Grant No.51101056) and National Science & Technology Pillar Program (Grant No.2011BEA12B03).

References

[1] Johansson TB, Kelly H and Reddy AN. *Renewable energy sources for fuel and electricity*. Beijing: Petroleum Industry Press; 2000.

[2] Gielen DJ, de Feber MAPC and Bos AJM. Biomass for energy or materials?: A Western European systems engineering perspective. *Energy Policy* 2001; **29**:291.

[3] Baxter LL, Miles TR, Miles TR Jr, Jenkins BM, Dayton D, Milne T, Bryers RW, Oden LL. The behavior of inorganic material in biomass-fired power boilers:field and laboratory experiences.*Fuel Processing Technology* 1998; **54**:47–78.

[4] Jensen PS, Stenholm M, Hald P. *Energy and Fuels* 1997;**11**:1048.

[5] Michelsen HP, Larsen OH, Frandsen F, Dam-Johansen K. Deposition and high temperature corrosion in a 10 MW straw fired boiler. *Fuel Processing Technology* 1998; **54**:95.

[6] Montgomery M and Larsen OH. Field test corrosion experiments in Denmark with biomass fuels. Part 2: Co-firing of straw and coal. *Materials and Corrosion* 2002; **53**:185.

[7] Liu C, Little J, Henderson PJ and Ljung P. Corrosion of TP347H FG stainless steel in a biomass fired PF utility boiler. *Journal of Materials Science* 2001; **36**:1015.

[8] Pettersson J, Pettersson C, Asteman H, Svensson JE and Johansson LG. A Pilot Plant Study of the Effect of Alkali Salts on Initial Stages of the High Temperature Corrosion of Alloy 304L. *Materials Science Forum* 2004; **461–464**:965.

[9] Grabke HJ. *Incinerating Municipal and Industrial Waste.* New York: Hemisphere Publishing; 1989.

[10] Grabke HJ, Reese E, Spiegel M. The effects of chlorides, hydrogen chloride, and sulfur dioxide in the oxidation of steels below deposits. *Corrosion Science* 1995; **37**:1023.

[11] Petterson J, Asteman H, Svensson JE, Johansson LG. KCl Induced Corrosion of a 304-type Austenitic Stainless Steel at 600°C; The Role of Potassium. *Oxidation of Metals* 2005; **64**:23–41.

[12] Jonsson T, Froitzheim J, Petterson J, Svensson JE, Johansson LG, Halvarsson M. The Influence of KCl on the Corrosion of an Austenitic Stainless Steel (304L) in Oxidizing Humid Conditions at 600 °C: A Microstructural Study. *Oxidation of Metals* 2009; **72**:213–239.

[13] Zahs A, Spiegel M and Grabke HJ. Chloridation and oxidation of iron, chromium, nickel and their alloys in chloridizing and oxidizing atmospheres at 400–700°C. *Corrosion Science* 2000; **42**:1093–1122.